Monte Carlo and Molecular Dynamics Studies of Interlayer Structure in $Li(H_2O)_3$−Smectites

Jeffery Greathouse*,†,‡ and Garrison Sposito†

Earth Sciences Division, Mail Stop 90/1116, Lawrence Berkeley National Laboratory, Berkeley, California 94720, and Department of Chemistry, University of the Incarnate Word, 4301 Broadway, San Antonio, Texas 78209

Received: November 7, 1997; In Final Form: January 22, 1998

Monte Carlo and molecular dynamics simulations were performed to elucidate interlayer structure in hydrated Li−smectites (hectorite, beidellite, or montmorillonite with interlayer Li^+) at low water content ($H_2O/Li = 3$). Previous spectroscopic studies of these stable clay mineral hydrates have led to interlayer structural models based on a postulated inner-sphere surface complex comprising Li^+ bound directly to the smectite surface while surmounted by exactly three solvating water molecules that execute hindered rotational motions. Our simulation results, based on tested water−water, Li^+−water, water−clay mineral, and Li^+−clay mineral potential functions, showed that the nature of the interlayer Li^+ solvation complexes in fact depends critically on the location of negative charge sites within the smectite layers. Inner-sphere surface complexes were observed to form exclusively on Li−beidellite (tetrahedral charge sites), outer-sphere surface complexes formed exclusively on Li−hectorite (octahedral charge sites), and both types of surface complex formed on Li−montmorillonite, which also contains both types of charge site. The Li^+ solvation number in these clay hydrates can vary from two to four. Rotational motions of the water molecules solvating Li^+ occurred (on a picosecond time scale) only if inner-sphere surface complexes had formed, again strongly contradicting the spectroscopic models. Improvement of these models and the spectroscopic data is needed to resolve the major differences between our simulation predictions and the current experimental interpretations of interlayer structure on $Li(H_2O)_3$−smectites.

Introduction

Lithium-saturated hectorite [$Li^+_{0.58}Si_8Mg_{5.42}Li_{0.58}O_{20}(OH,F)_4$], a trioctahedral 2:1 clay mineral,[1] exhibits a stable interlayer hydration state for water adsorbed at half-monolayer coverage, corresponding to an average of three water molecules per interlayer Li^+ ($H_2O/Li = 3$).[2] Spectroscopic study of this hydrate, $Li(H_2O)_3$−hectorite, has long been a challenging experimental conundrum,[3] accentuated by the strong competition that exists between water molecules and siloxane surface oxygen ions for coordination about the Li^+ counterions. A trihydrate complex, $Li(H_2O)_3^+$, has been documented for concentrated LiCl solutions ($H_2O/Li < 6$).[4] It is possible, therefore, that a stable trihydrate configuration could exist on the siloxane surfaces of $Li(H_2O)_3$−hectorite.[2,3]

Prost[2,5,6] investigated the configuration of water molecules in $Li(H_2O)_3$−hectorite by IR absorption spectroscopy, applying the technique of progressive deuteration to the adsorbed water molecules in order to decouple their normal-mode vibrations. An IR-active band was observed at 3610 cm^{-1} for the hydroxyl group in HOD, while the stretching−vibration bands of HOH were observed at 3580 cm^{-1} (ν_s) and 3640 cm^{-1} (ν_{as}). The asymmetric stretching band exhibited dichroism that was consistent with an orientation of one adsorbed-water OH almost perpendicular to the siloxane surface. Prost[2,6] postulated that a stable trihydrate surface complex existed in the hectorite interlayer region, with Li^+ residing at the apex of an inverted pyramid whose base comprised the three solvating water molecules, each of which retains its C_{2v} symmetry (Figure 1). (A perfect orientation of the water OH perpendicular to the siloxane surface would decrease slightly the 55° angle, shown in Figure 1, to 52.5°.)

Poinsignon et al.[7] confirmed the two HOH IR stretching bands observed by Prost,[2] interpreting their significantly lower values relative to the corresponding bands for water vapor ($\nu_s = 3657$ cm^{-1}, $\nu_{as} = 3756$ cm^{-1}) as the effect of strong polarization of the solvating water molecules by the electric field of Li^+. A model calculation of the net polarizing force created by Li^+ showed it to be directed approximately along a water OH, which implies that the Li^+−H_2O line of centers is also collinear with a water OH. By contrast, in the Prost[2,6] model (Figure 1), the Li^+−H_2O line of centers is congruent with the C_2 axis of the water molecule, as is found also in ab initio calculations of the structure of the Li^+−H_2O solvation complex.[8] If the model of Poinsignon et al.[7] is correct, it is the transition dipole moment vector M_{as} that would be perpendicular to the siloxane surface in Figure 1, not a water OH group, and granting accuracy to the polarization hypothesis of Poinsignon et al.,[7] an orientation of the solvating water molecules as in Figure 1 should result in no red shift of ν_{as} from the value for water vapor, because the transition dipole moment vector M_{as} is perpendicular to the electric field created by Li^+. However, the red shift observed for the two HOH stretching bands of adsorbed water in $Li(H_2O)_3$−hectorite need not result solely from strong polarization of the solvating water molecules by Li^+. Red shifts could be

† Lawrence Berkeley National Laboratory.
‡ University of the Incarnate Word.
* Address correspondence to this author at the e-mail address greathou@universe.uiwtx.edu.

S1089-5647(98)00120-5 CCC: $15.00
Published on Web 03/06/1998

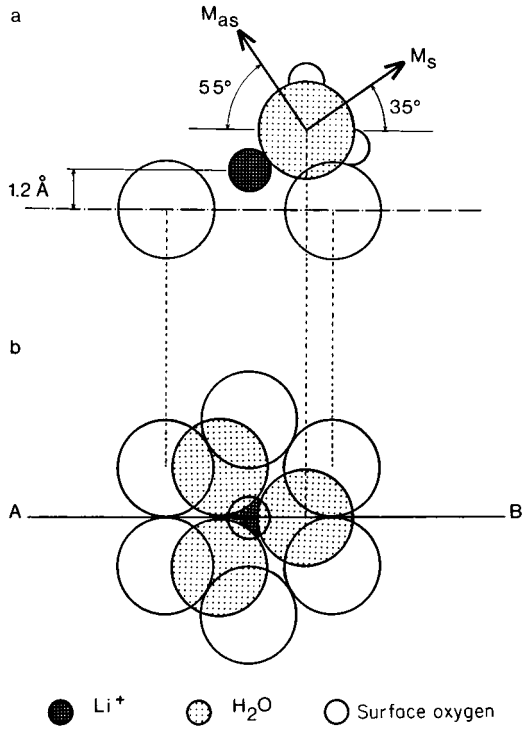

Figure 1. Prost[2] model of the trihydrate inner-sphere surface complex in $Li(H_2O)_3$−hectorite. Stipled circles denote water oxygens, open circles are siloxane surface oxygens, and the crosshatched circle is Li^+. The transition dipole moment vectors for IR-active symmetric and asymmetric stretching vibrations are denoted M_s and M_{as}, respectively. Upper view (a) is in the (z,x) plane and lower view (b) in the (y,x) plane.

produced by H bonding to the siloxane surface, a point also recognized by Poinsignon et al.[7]

The vibrationally averaged configuration[3] of the adsorbed water molecules in $Li(H_2O)_3$−hectorite was investigated by Conard et al.[9] and Poinsignon et al.[10] using quasielastic neutron scattering (QNS) spectroscopy. No elastic scattering from water molecules that remained stationary on the QNS time scale was observed in their spectra, in agreement with earlier QNS studies of low-order Li−smectite hydrates.[3] The quasielastic spectral width was consistent with a site residence time for adsorbed water molecules that was on the order of 100 ps.[10] The full quasielastic spectrum was modeled as a convolution of translational diffusion of individual water molecules, rotational diffusion of a $Li(H_2O)_3^+$ surface complex around a C_3 axis perpendicular to the siloxane surface (cf. Figure 1), and rotation of the H−H line of centers in a solvating water molecule around its C_2 axis, which was taken to be perpendicular to the C_3 axis of the trihydrate complex. Correlation times (τ_2) for the two types of rotation differed by an order of magnitude, with τ_2 for the faster C_2 rotation being comparable to τ_2 for the C_2 rotations of water molecules in the first solvation shell of Li^+ in aqueous solution (i.e., 2−3 ps).[11] This dynamic picture of the vibrationally averaged trihydrate structure implies that significant anisotropy will exist in the QNS spectrum because of the fixed orientations of the C_3 and C_2 axes on the QNS time scale. Weak anisotropy was indeed confirmed for the C_3 rotational contribution to the QNS spectrum,[9,10] but not for the C_2 rotational contribution. Conard et al.[9] then speculated that this latter result was the effect of oscillation of the adsorbed Li^+ between two sites located about 1 Å apart along the C_3 axis, near each opposing siloxane surface. This spectrum-blurring oscillation evidently would occur on the QNS time scale (ca. 100 ps) and, therefore, would not contradict the vibrational-band dichroism that occurs on the much shorter IR time scale (ca. 10^{-2} ps).

Conard[12,13] and Fripiat et al.[14] investigated the diffusionally averaged configuration[3] of the counterion surface complexes in $Li(H_2O)_3$−hectorite using ^1H, ^2H, and ^7Li NMR spectroscopies. The variation of ^1H and ^2H Pake doublets with changes in orientation of the applied magnetic field was interpreted[14] in terms of a $Li(H_2O)_3^+$ surface complex in which the H−H line of centers of the water molecules each are perpendicular to their C_2 axes, while the C_2 axes make an angle of 70 ± 2° with the C_3 axis of the trihydrate [as opposed to 90° in the model used to interpret QNS spectra[9,10] and 55 ± 3° in the Prost[6] model (Figure 1)]. Pake doublet variations in the ^2H NMR spectra were ratioed to those in the ^1H NMR spectra to yield 62 ± 1° as the angle between the C_2 axis and the symmetry axis of the electric field gradient in ^2H_2O. This angle would be 52° in the model of Poinsignon et al.,[7,10] whereas it is near 0° in the Prost[6] model (Figure 1). Fripiat et al.[14] speculated that an imprecise estimate of either the quadrupole coupling constant for ^2H or the $^2HO^2H$ angle (because of strong water molecule polarization by Li^+) could account for the difference between their model calculation and the 52° angle necessary for the ^2H_2O electric field gradient to be directed along an O^2H bond.[7] Measurements of the spin−lattice relaxation time made in pulsed ^1H NMR experiments led Fripiat et al.[14] to estimates of the correlation times for the C_3 and C_2 rotations that differed by 2 orders of magnitude (larger) from those obtained by the analysis of QNS spectra.[9,10]

The doublet line shape observed in the ^7Li NMR spectrum of $Li(H_2O)_3$−hectorite[12,13] conformed to that expected for an axially symmetric electric field gradient in Li^+. This electric field gradient decreased as the water content was increased from half-monolayer toward monolayer coverage, an effect observed also by Luca et al.[15] in their ^{23}Na and ^7Li NMR spectra of the low-order hydrates of the dioctahedral 2:1 smectite, montmorillonite.[1] The magnitude of the ^7Li doublet splitting (proportional to the electric field gradient in Li^+), however, was considerably smaller than that expected for a Li−O distance of 1.95 Å, which is that observed for the $Li(H_2O)_3^+$ complex in concentrated aqueous solutions.[4] The observed doublet splitting implied instead a much larger Li−O distance of 2.45 Å.

Significant differences thus exist among the several model constructs that have emerged from spectroscopic studies to describe the local configuration of water molecules adsorbed on $Li(H_2O)_3$−hectorite.[6,7,9,13] A principal contentious issue is the relative orientation of the C_2 axis of the water molecules, both with respect to the siloxane surface of the clay mineral and with respect to the electric field of the Li^+ counterion. In Figure 1, the C_2 axis makes an angle of 125° (strictly, 128°) as measured counterclockwise from a normal to the siloxane surface (the supplement of the 55° angle shown in Figure 1), and it makes an angle near 0° with the electric field created by Li^+, which is positioned over a siloxane surface ditrigonal cavity about 1.2 Å further into the interlayer region than are the centers of the surrounding surface oxygen ions. In the model of Conard−Poinsignon,[7,9,10] the C_2 axis makes a right angle as measured counterclockwise from a normal to the siloxane surface (cf. Figure 7 in Sposito and Prost[3]) and makes an angle of about 52° with the Li^+−H_2O line of centers as measured in a clockwise direction. In the model of Fripiat et al.,[14] the C_2 axis makes an angle of 110° as measured counterclockwise from a normal to the siloxane surface and an angle of 62° as measured clockwise from the Li^+−H_2O line of centers, the Li^+ ion then

being positioned about 2.1 Å further into the interlayer region than are the centers of the surface oxygen ions.[14]

Neither counterions nor adsorbed water molecules diffuse on the very short IR time scale, whereas both diffuse on the NMR time scale, and the water molecules diffuse while the counterions merely oscillate on the QNS time scale—all of which adds complexity to the problem of reconciling the foregoing conceptual differences concerning the issues of water molecule orientations, the small electric field gradient in Li^+, or the isotropicity of water molecule rotations on the QNS time scale. In these circumstances, research on molecular behavior in aqueous solutions has long benefited from guiding insights provided by Monte Carlo (MC) and molecular dynamics (MD) simulations.[11,16,17] Comparison of the simulation results with experiment not only tests the accuracy with which molecular interactions have been described but also points the way to the new experiments needed to resolve differences in conceptualization.[18] In this paper, interlayer molecular structure in the $Li(H_2O)_3$−hectorite hydrate is investigated by MC and MD simulations based on tested water−water, Li^+−water, water−clay mineral, and Li^+−clay mineral potential functions.[19] Our MC/MD codes and phase-space sampling strategies have been applied successfully to the one-, two-, and three-layer hydrates of both Li− and Na−montmorillonite,[19,20] as well as to other hydrated trioctahedral and dioctahedral smectites.[21−23] The predictions made of basal-plane spacings, of interlayer molecular structure and adsorbed species mobilities, and of counterion speciation all have been in good agreement with available experimental data,[19−23] thus encouraging an application of our approach to a strongly interacting clay hydrate system, such as $Li(H_2O)_3$−hectorite. The objectives of our study were to examine the competition between adsorbed water molecules and clay mineral surface oxygen ions for coordination to Li^+ counterions, as well as to evaluate the trihydrate surface complex models that have been proposed for $Li(H_2O)_3$−hectorite solely on the basis of spectroscopic evidence.

Methods

Poinsignon et al.[10] extended their QNS measurements to investigate Li−montmorillonite and Li−vermiculite[1] bearing one monolayer of adsorbed water, concluding from their data analysis that the dynamic Li−trihydrate concept of Conard[13] applied to these two clay minerals as well. Therefore, in the spirit of evaluating the trihydrate surface complex model as comprehensively as possible, MC/MD simulations were performed for hydrates of three Li−smectites:

Hectorite: $Li_{0.75}[Si_8](Mg_{5.25}Li_{0.75})O_{20}(OH)_4$

Montmorillonite (Wyoming-type): $Li_{0.75}[Si_{7.75}Al_{0.25}](Al_{3.5}Mg_{0.5})O_{20}(OH)_4$

Beidellite: $Li_{0.75}[Si_{7.25}Al_{0.75}](Al_4)O_{20}(OH)_4$

the first being a trioctahedral 2:1 clay mineral, whereas the second two are dioctahedral 2:1 clay minerals.[1] The three smectite unit-cell formulas do not differ in respect to layer charge ($x = 0.75$) but instead are distinguished by their isomorphic substitution patterns, [ ] referring to the two tetrahedral sheets and ( ) to the octahedral sheet. Hectorite has octahedral charge substitution only, whereas beidellite has tetrahedral charge substitution only, like vermiculite, but with about half the layer charge of the latter clay mineral.[1]

Simulation methods followed closely those described in detail by Chang et al.[19] for low-order Li−montmorillonite hydrates. Briefly, each simulation cell contained approximately eight unit cells of the clay mineral, resulting in a 21.12 by 18.28 Å patch in the (x,y) plane. The simulation cell was arranged so that the center of the octahedral sheet in the clay mineral layer was located at the bottom (or top) of the cell. Three-dimensional periodic boundary conditions were used, producing an infinite stack of clay layers. Artifacts deriving from the imposition of infinite periodicity were obviated by utilizing a real space cutoff (<9 Å) in the all-image convention for short-range interactions, while applying the Ewald sum method with a reciprocal space cutoff ($k < 3$ Å^{-1}) to represent long-range Coulomb interactions beyond the real space cutoff distance. Charge sites were created by reducing the electrostatic charge of a cationic clay layer site by 1.0 protonic charge. Substitution sites were selected so that a regular three-dimensional array of charge sites was not created. The simulation cell comprised six Li^+ ions and 18 water molecules, corresponding to a water content of approximately 55 g of water/kg of clay. All intermolecular and interatomic interactions (clay−clay, clay−water, clay−ion, water−ion, water−water, and ion−ion) were described by MCY model-based interaction parameters.[19−24] Being derived from ab initio calculations on water dimers, the MCY model does not mimic the extent of tetrahedral coordination that is observed in bulk liquid water.[16] However, for simulating the perturbed water structure in the constrained geometric environment offered by clay interlayers, this model has been successful[19,20] in predicting both thermodynamic quantities (layer spacing and water potential energy) and interlayer species mobilities that compare very well with experiment.

Monte Carlo simulations were performed in an (N,σ,T) ensemble using the computer code MONTE,[25] in which the applied stress normal to the clay mineral basal planes (σ_{zz}) is fixed at 100 kPa and $T = 300$ K. Initially, the layer spacing was set at 12.0 Å, with Li^+ counterions arranged at the midplane directly above or below a charge site. This initial placement of ions expedites convergence to MC equilibrium.[19,20] Water molecules were placed randomly in the interlayer region, and during the first 25 000 simulation steps, they were the only species allowed to move. During the next 25 000 steps, water molecules and the clay mineral layers were allowed to move, after which all interlayer species were allowed to move until equlibration was achieved. The clay mineral c-axis was also allowed to move one step in any direction for approximately every five cycles of interlayer species movements. (For six cations and 18 water molecules, one cycle is equal to 24 steps.) Monte Carlo equilibration was judged by monitoring the convergence profiles of the layer spacing and intermolecular potential energy.[19,20,24] Data were collected at 500-step intervals for at least another 300 000 steps after MC equilibrium was attained.

Equilibrium MC configurations with intermolecular potential-energy and layer-spacing values close to the average (within 0.1 Å for the layer spacing) were used as starting configurations in the MD simulations. Molecular dynamics simulations then were performed in an (N,V,E) ensemble using the computer code MOLDY,[26] keeping the simulation cell axes (a,b,c) fixed throughout. Initial velocities were randomly assigned from a Maxwell−Boltzmann distribution, and the temperature was scaled for the first 5.0 ps of each simulation. The MD runs were 200 ps in length, with a time step of 0.5 fs. Data were collected every 100 time steps.

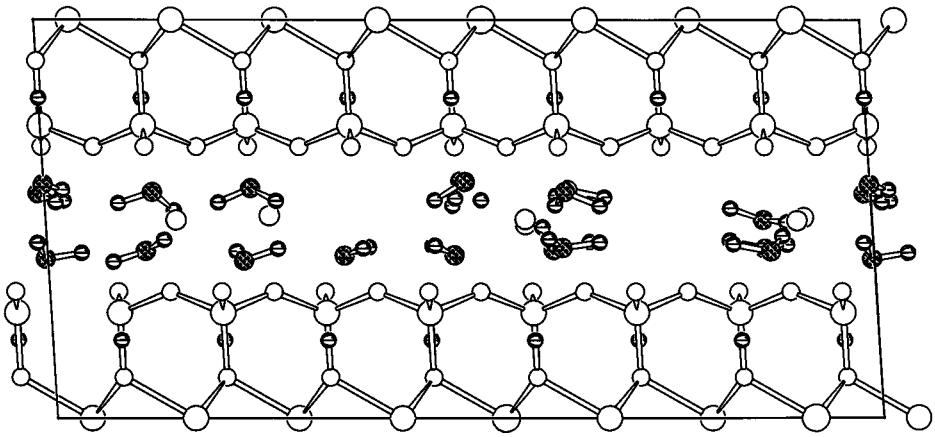

Figure 2. MC snapshot of the interlayer configuration in $Li(H_2O)_3$−hectorite as seen in the (*z*,*x*) plane. Counterions are shown as single disks.

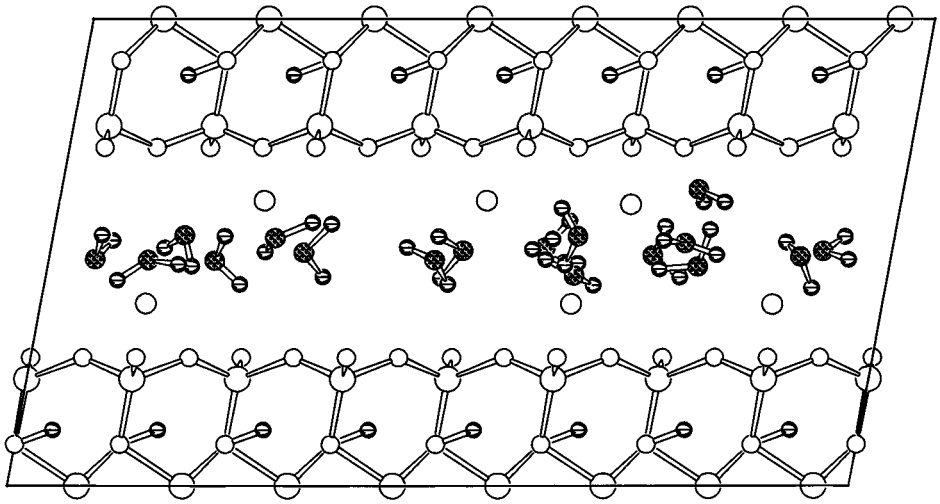

Figure 3. MC snapshot of the interlayer configuration in $Li(H_2O)_3$−beidellite as seen in the (*z*,*x*) plane. Counterions are shown as single disks.

Results

Monte Carlo Simulations. The MC simulations of $Li(H_2O)_3$−hectorite and $Li(H_2O)_3$−montmorillonite equilibrated after a few hundred thousand steps, whereas $Li(H_2O)_3$−beidellite required nearly 1 million steps for MC equilibration. This much longer equilibration time resulted from sluggish Li^+ migration out of their initial midplane positions to the tetrahedral charge sites located on the beidellite basal planes (ca. 800 000 steps), as well as from significant equilibration shifts of the cell *c*-axis coordinates in the *x*−*y* plane (ca. 15 000 steps). The average MC equilibrium layer spacing for the three hydrates increased with the fraction of layer charge assigned to tetrahedral sites: 10.32 ± 0.04 Å (hectorite, 600 000 steps), 11.40 ± 0.05 Å (montmorillonite, 600 000 steps), 11.93 ± 0.07 Å (beidellite, 1 800 000 steps). Experimental data with which to compare these predictions are rare, since most XRD studies do not examine the layer spacing of Li−smectites at very low water content. Exceptions to this trend are the detailed XRD data of Calvet[27] and, more recently, Bérend et al.[28] for Li−montmorillonite hydrates. At a water content of 50 g of water/kg of clay, Bérend et al.[28] reported 11.3 Å as the layer spacing for Li−montmorillonite (desorption isotherm), which is consistent with our MC result. By contrast, most papers on Li−hectorite hydrates merely cite a layer spacing of 12 Å, the value expected for a full-monolayer hydrate,[5,14] as that for the half-monolayer hydrate as well.

Figures 2−4 show representative "snapshots" of the interlayer molecular configuration for $Li(H_2O)_3$−hectorite, −beidellite, and −montmorillonite, respectively. These snapshots indicate at a glance that the distribution of interlayer species differs dramatically among the three clay mineral hydrates. For hectorite (Figure 2), only outer-sphere surface complexes form, leaving all Li^+ to reside at the interlayer midplane with water molecules interposed between them and the opposing siloxane surfaces. The same surface speciation was observed by Skipper et al.[29] for Na^+ counterions in MC simulations of the monolayer hydrate of Otay-type montmorillonite, a dioctahedral smectite having only octahedral charge sites. By contrast, inner-sphere surface complexes are the sole interlayer species of Li^+ on beidellite (Figure 3), with the counterions now residing directly over the tetrahedral charge sites and the water molecules relegated to the midplane. Skipper et al.[29] observed the same result for Na^+ in MC simulations of the monolayer hydrate of vermiculite (layer charge $x = 1.5$), a trioctahedral clay mineral having only tetrahedral charge sites.[1] Predictably, Wyoming-type montmorillonite, which has both tetrahedral and octahedral charge sites,[1] exhibits both inner-sphere and outer-sphere surface complexes (Figure 4). Similar results in MC simulations were reported for Na^+ and Li^+ counterions in low-order hydrates of Wyoming-type montmorillonite by Skipper et al.,[29] Chang et al.,[19,20] and Boek et al.[30]

Lithium−oxygen and Li−H radial distribution functions (RDF) for the three smectite hydrates (data not shown) featured sharp nearest-neighbor peaks at 1.95−2.00 and 2.3−2.5 Å, respectively, in very good agreement with the Li−O (1.95 ± 0.02 Å) and Li−H (2.50 ± 0.02 Å) distances that have been

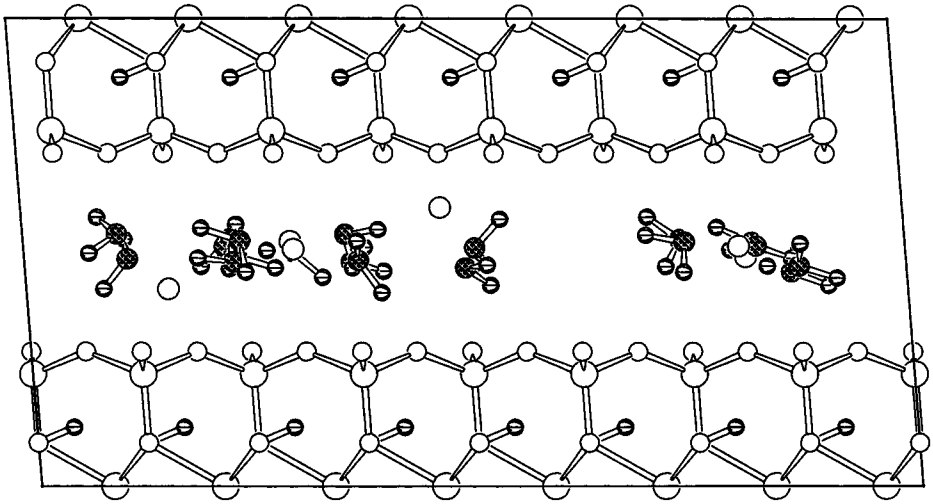

Figure 4. MC snapshot of the interlayer configuration in $Li(H_2O)_3$−montmorillonite as seen in the (z,x) plane. Counterions are shown as single disks.

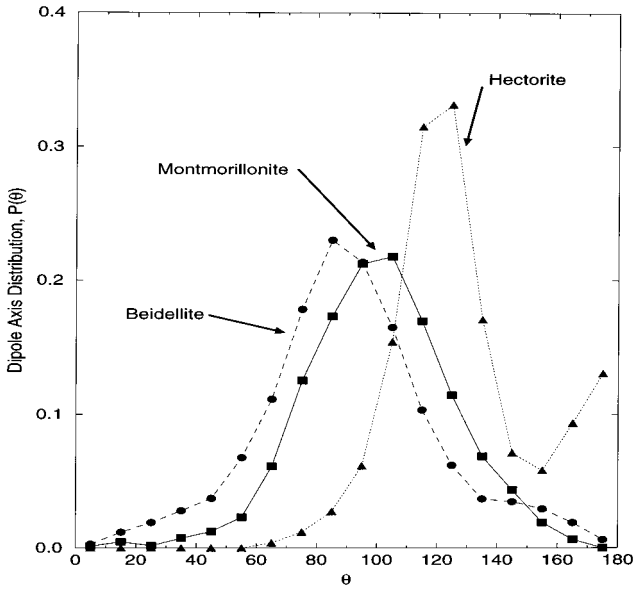

Figure 5. Unnormalized distribution of the angle (θ) measured clockwise between the dipole moment vector of a water molecule and a line perpendicular to the nearest siloxane surface.

determined experimentally by neutron isotopic-difference diffraction for the $Li(H_2O)_3^+$ trihydrate complex in concentrated LiCl solutions.[4] The O−O and intermolecular H−O RDF (data not shown) exhibited first-neighbor peaks at 2.3−2.6 and 2.0−2.5 Å, respectively. These positions differ significantly from the corresponding values found for MCY bulk water (2.8 and 1.9 Å).[24]

Insight into the interlayer hydrate structure also can be obtained by examination of the distribution of the angle (θ) measured clockwise between the dipole moment vector of a water molecule (congruent with the vector M_s in Figure 1) and a line normal to the nearest siloxane surface.[29] [The dipole moment orientation angle, θ, thus is equal to the supplement of the angle between the transition dipole moment vector M_{as} and the siloxane surface.] Figure 5 shows this distribution [$P(\theta)$, which has not been normalized to the solid angle through division by sin θ] for the three Li−smectite hydrates. Broad neighboring peaks, centered near $\theta \approx 85°$ and 105°, are evident for beidellite and montmorillonite, respectively, whereas hectorite exhibits a strong peak near $\theta \approx 125°$, with additional but subordinate density arising near $\theta \approx 180°$. The beidellite and montmorillonite $P(\theta)$ peaks are consistent with water molecules oriented so that their C_2 axes are nearly parallel to the siloxane surface (an orientation noted also by Chang et al.[20] for the monolayer hydrate of Li−montmorillonite), while water OH are each directed toward a siloxane surface (cf. Figures 3 and 4). The principal hectorite peak, on the other hand, is consistent with an orientation of the C_2 axis like that of the water molecule in Figure 1—but in hectorite the Li^+ counterion resides in the midplane, not at the siloxane surface (Figure 2). The noticeable growth in $P(\theta)$ near $\theta \approx 180°$ is consistent with some water molecules orienting their dipole moment vectors perpendicularly to the nearest basal plane pointing into the interlayer region. These water molecules are not hydrating the Li^+ counterions (cf. Figure 2).

Molecular Dynamics Simulations. Our MD simulations extended to 200 ps, which overlaps with the QNS time scale, thus giving dynamical information related to the vibrationally averaged configuration of water molecules in the interlayer region.[3] Figure 6 shows cumulative center-of-mass trajectories of selected Li^+ and H_2O in hectorite, projected onto the (z,x) plane and monitored over 200 ps. The labeled values of z and x are distances measured from the center of the simulation cell, the interlayer midplane corresponding to $z = 0$. The trajectory plots, which are representative of all cations in the $Li(H_2O)_3$−hectorite interlayer region, reveal oscillatory motions of Li^+ along an axis normal to the siloxane surface, the oxygen ions of which, although not shown, are centered on the planes defined by $z = \pm 1.88$ Å. The amplitude of the Li^+ oscillations is about 0.5 Å. Jump movement of Li^+ along the x-direction is also apparent in Figure 6. This movement represents cation hopping between adjacent sites over surface oxygen ions located above the (octahedral) charge sites in hectorite. Oscillations of the water molecules along the z-direction between $z = \pm 0.3$ Å and $z = \pm 1.3$ Å are evident in Figure 6, but there is no significant lateral movement, because these molecules are hindered from doing so by the boundaries of the ditrigonal cavities in the siloxane surface (cf. Figure 2).

Limited excursion of Li^+ bound to a tetrahedral charge site in the interlayer region of $Li(H_2O)_3$−beidellite was observed in center-of-mass trajectory plots, with the vicinal three water molecules hovering loosely at the midplane (data not shown). Not surprisingly, trajectory plots for Li^+ and H_2O in the interlayer region of $Li(H_2O)_3$−montmorillonite (Figure 7) are approximately superpositions of those for Li−hectorite near

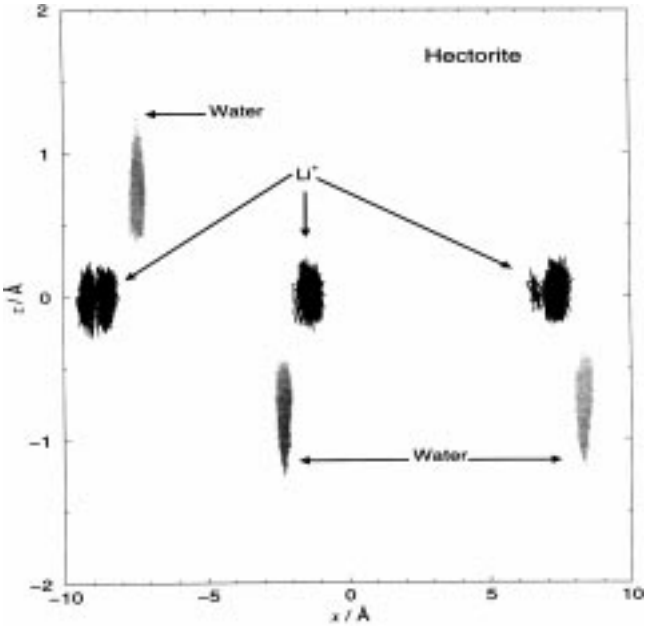

Figure 6. MD simulation of the cumulative trajectories (over 200 ps) of Li^+ (black) and three hydrating water molecules (gray) as seen in the (*z*,*x*) plane on hectorite.

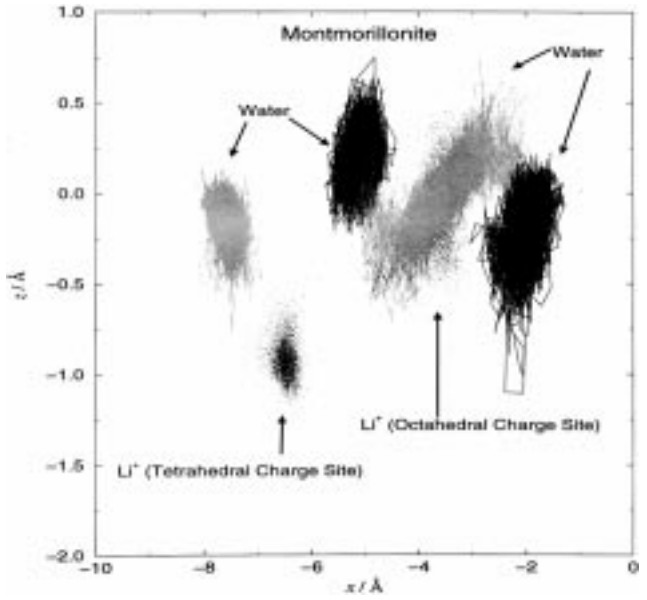

Figure 7. MD simulation of the cumulative trajectories (over 200 ps) of Li^+ (stipled) and three hydrating water molecules (gray or black) as seen in the (*z*,*x*) plane on montmorillonite.

octahedral charge sites and those for Li−beidellite near tetrahedral charge sites. The much larger amplitude of oscillation seen for Li^+ near an octahedral charge site in montmorillonite (ca. 1.0 Å), as compared to hectorite, is a result of water molecules now sharing the midplane with Li^+, thus leaving more space in which to move near the siloxane surface that is opposite an octahedral charge site.

Rotations of the interlayer water molecules about their C_2 axes are equivalent to periodic changes in the positions of the water protons that, in turn, can produce time dependence in the angle (ψ) that a vector through the H−H line of centers makes with a line normal to the siloxane surface nearest to the rotating water molecule.[20,29] Monte Carlo calculation of the distribution of ψ-values among the water molecules in the interlayer region of $Li(H_2O)_3$−hectorite (data not shown) showed a strong, narrow peak near 90°, corresponding to an H−H vector that is nearly parallel with the siloxane surface (cf. Figure 2) and whose rotation in this case would not lead to a change in ψ. (Inversion of the direction of a vector through the H−H line of centers produces a ψ-value that is the supplement of the initial value.) About two-thirds of the water molecules in $Li(H_2O)_3$−hectorite, in fact, displayed no systematic change in the positions of the water protons that would indicate any kind of rotation during the 200 ps MD simulation (data not shown). The remaining third of the water molecules did show an erratic rotation during 200 ps (Figure 8). They were the water molecules keyed into the ditrigonal cavities of the siloxane surfaces. By contrast, the MC distribution of ψ-values for water molecules in $Li(H_2O)_3$−beidellite exhibited a very broad peak, extending from 15° to 55° (data not shown), but with evident erratic rotation of the water molecules during 200 ps (Figure 9). About two-thirds of the water molecules in $Li(H_2O)_3$−montmorillonite, whose MC distribution of ψ-values was broadly and symmetrically peaked at 45° (data not shown), produced a systematic rotational pattern like that shown in Figure 10. This pattern, corresponding to a calculated average proton residence time of ca. 100 ps, was observed for the water molecules hydrating Li^+ bound to both tetrahedral and octahedral charge sites.

Discussion

$Li(H_2O)_3$−Hectorite. Figure 11 gives a typical MC snapshot of the interlayer configuration in $Li(H_2O)_3$−hectorite, as seen in projection onto the siloxane surface. (The simulation cell is outlined with a solid line, and the upper clay layer has been deleted to facilitate viewing.) Striking differences are apparent between the interlayer hydrate structure in this figure and the trihydrate model that has been inferred from spectroscopic measurements.[6,9,13] The Li^+ are seen to form outer-sphere surface complexes exclusively, thus residing at the interlayer midplane (cf. Figure 2), in sharp disagreement with the inner-sphere surface complex that was proposed to model spectroscopic data.[2,10,12] Moreover, the solvation number of each Li^+ is not uniformly equal to three, as assumed a priori in the spectroscopic models, but instead is equal to two, with the remaining water molecules being tucked into the ditrigonal cavities of the siloxane surfaces, evidently attracted there by structural protons that lie below in the octahedral sheet (cf. the vertically oriented structural OH in Figure 2). Of course, no trihydrate C_3 rotational motion appears in the MD simulation dynamics of the configuration in Figure 10, because there are no trihydrate surface complexes. Rotation of the interlayer water molecules around their C_2 axes does occur on the MD time scale (200 ps) for the water molecules keyed into the surface ditrigonal cavities, but they do not solvate Li^+. (One such molecule is at the center of the simulation cell in Figure 11.)

The hydrate structure shown in Figure 11 is consistent with dichroism in the asymmetric HOH stretching−vibration band, as observed by IR spectroscopy,[2] and for the water molecules that do solvate Li^+, it exhibits precisely the average dipole moment vector orientation ($\theta \approx 125°$ at the peak in Figure 5, equivalent to the 55° angle indicated in Figure 1) that was deduced by Prost[2] from dichroic IR spectral behavior. Polarization by Li^+ and weak H bonding of the water molecules to the siloxane surface evidently contribute together to cause the observed IR red shift in the HOH stretching bands.[2,5,7] On the MD time scale, the interlayer Li^+ oscillate along the *c*-axis (Figure 6), as was proposed by Conard et al.[9] to explain the lack of anisotropicity in their high-wavelength QNS spectra. The Li^+ engage in lateral hops on this time scale as well, consistent with the absence of any elastic peak in the QNS

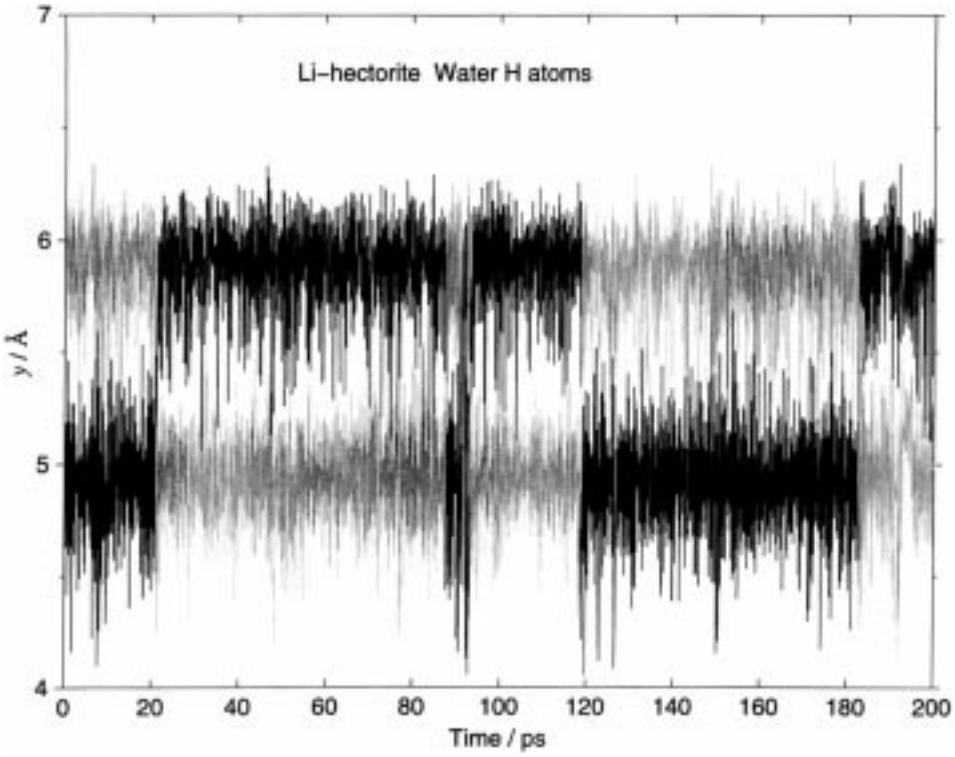

Figure 8. MD simulation of the time dependence of the *y*-coordinates (denoted in either gray or black) of a pair of protons in a water molecule keyed into a ditrigonal cavity of the hectorite surface. Note the sporadic exchanges of *y*-coordinates, indicating that rotations of the H−H line of centers are occurring.

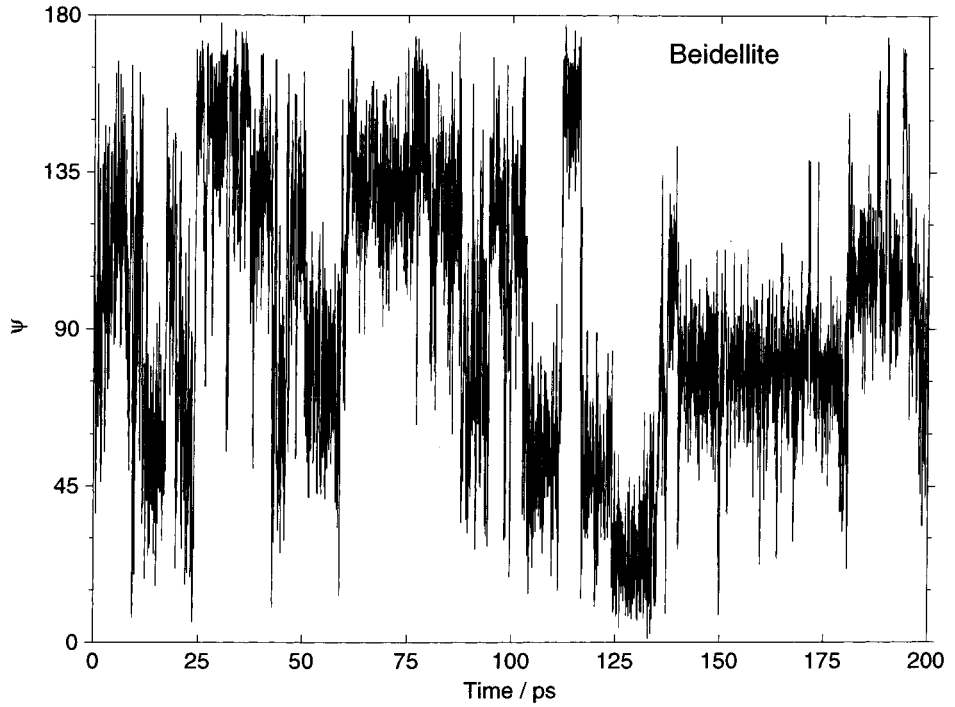

Figure 9. Time dependence of the angle (ψ) between a vector through the H−H line of centers of a rotating water molecule and a line perpendicular to the nearest siloxane surface (beidellite).

spectrum from hydrating interlayer water protons.[3,9,10] The weak anisotropicity in the low-wavelength QNS spectra reported by Conard et al.[9] may have resulted from sympathetic oscillatory motions of the interlayer water molecules along the *c*-axis, which also occurs on the MD time scale (Figure 6). On the much longer NMR time scale, exchange among the water molecule positions in Figure 11 will occur, leading to a diffusionally averaged, symmetric electric field gradient in Li^+, but with its value reflecting the presence of a much greater separation (3.0 Å) between Li^+ and the nearest nonsolvating water molecule, as compared to the two solvating water molecules (1.95 Å). The weighted-average $Li-H_2O$ distance is thus 2.3 Å, in reasonable agreement with the value 2.45 Å that was inferred from the measured electric field gradient.[12] The very large quantitative discrepancy between rotational correlation times as measured by QNS versus NMR spectroscopy[10,14] may well be

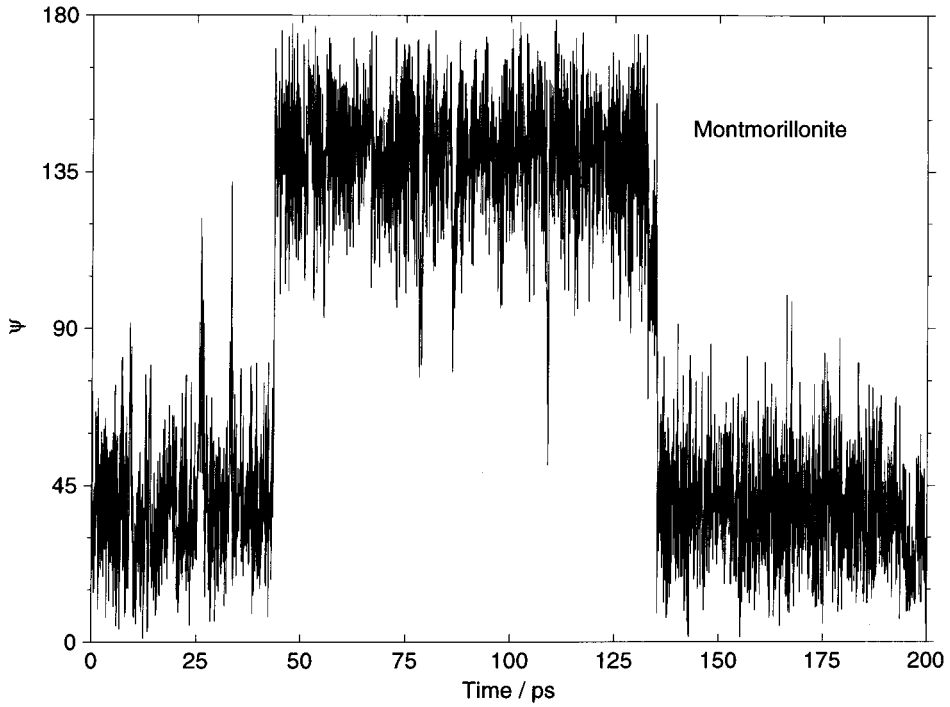

Figure 10. Time dependence of the angle (ψ) between a vector through the H−H line of centers of a rotating water molecule and a line perpendicular to the nearest siloxane surface (montmorillonite).

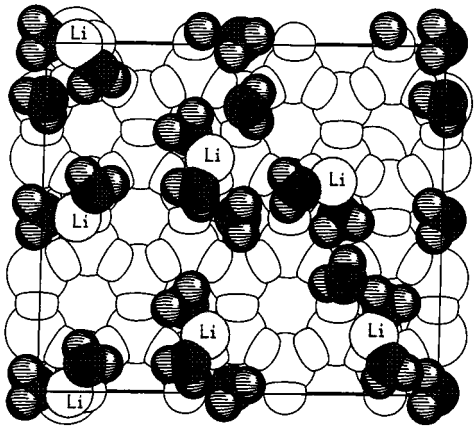

Figure 11. MC snapshot of the interlayer configuration in $Li(H_2O)_3$−hectorite as seen in the (y,x) plane.

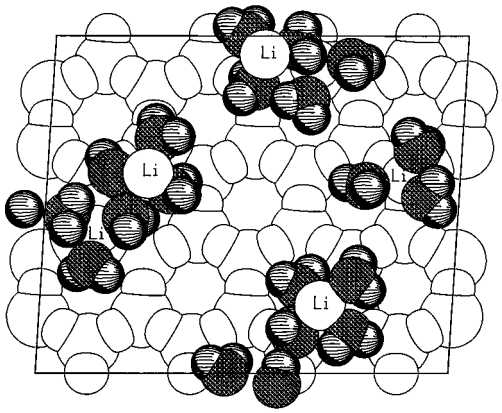

Figure 12. MC snapshot of the interlayer configuration in $Li(H_2O)_3$−beidellite as seen in the (y,x) plane.

symptomatic of the complete failure of the trihydrate inner-sphere surface complex model to describe the bihydrate outer-sphere surface complexes in $Li(H_2O)_3$−hectorite shown in Figure 11.

$Li(H_2O)_3$−Beidellite. Figure 12 shows a MC snapshot of the interlayer configuration in $Li(H_2O)_3$−beidellite as seen in projection onto the siloxane surface. The Li^+ form inner-sphere surface complexes with the siloxane ditrigonal cavities, just as portrayed in Figure 1, but the orientation of the hydrating water molecules is rather like that proposed by Conard−Poinsignon[7,9,10] ($\theta \approx 85°$, as opposed to $\theta \approx 125°$ in Figure 1), with the two OH bonds thus pointing toward opposing siloxane surfaces more equably than in Figure 1. On the MD simulation time scale, the Li^+ rattle about tetrahedral charge sites near the siloxane cavity while the solvating water molecules, which may number either two, three, or four, hover near the interlayer midplane. There was no discernible rotation of the surface complexes on this time scale, even for the Li^+ whose solvation number is three, whereas an erratic C_2 rotation of the solvating water molecules does occur (Figure 9). The hydrate structure for $Li(H_2O)_3$−beidellite thus resembles fairly closely that proposed first in order to model IR,[2] QNS,[9] and NMR[12] spectra of $Li(H_2O)_3$−hectorite and then extended by Poinsignon et al.[10] to Li−vermiculite, a trioctahedral clay mineral having only tetrahedral charge sites, similar to beidellite.

$Li(H_2O)_3$−Montmorillonite. Figure 13 provides a MC snapshot of $Li(H_2O)_3$−montmorillonite as seen in projection onto the siloxane surface. The speciation of Li^+ is mixed among inner-sphere surface complexes near tetrahedral charge sites and outer-sphere surface complexes near octahedral charge sites. The solvation number varies from two to four, and unlike the trioctahedral clay mineral, hectorite, there are no water molecules keyed into the siloxane ditrigonal cavities of the clay mineral in search of structural protons, evidently because of their significant inclination away from perfect alignment along the c-axis (cf. Figure 4). The solvating water molecules orient their dipole moment vectors roughly parallel with the siloxane surfaces ($\theta \approx 105°$) while rotating about their C_2 axes on a 100 ps time scale (Figure 10). There is no wholesale rotation of any Li^+ surface complex, regardless of its solvation number, on the MD time scale.

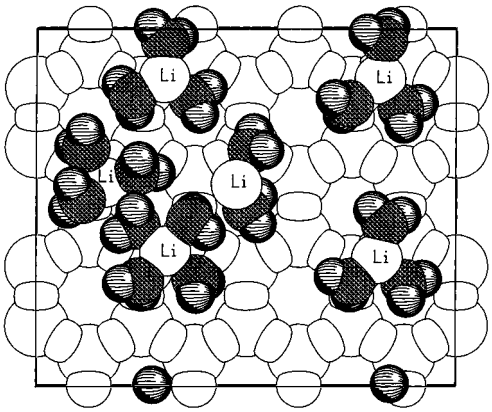

Figure 13. MC snapshot of the interlayer configuration in $Li(H_2O)_3$−montmorillonite as seen in the (y,x) plane.

Conclusions

Our MC/MD simulations of interlayer molecular configurations in $Li(H_2O)_3$−smectites indicate clearly that the trihydrate inner-sphere surface complex, proposed originally for $Li(H_2O)_3$−hectorite[2,6] and extended to other 2:1 clay minerals[10] on the basis of spectroscopic data, was an oversimplification in several respects. First, both inner-sphere and outer-sphere surface complexes are possible, depending on the type of surface charge site, and the Li^+ solvation number can vary from two to four. Second, rotational motions of these surface complexes are restricted to those of the water protons around C_2 axes (at least over a 200 ps time scale), and even these rotations are absent when outer-sphere surface complexes of Li^+ occur exclusively in the interlayer region (hectorite). Water molecules in $Li(H_2O)_3$−hectorite that are not in surface complexes with Li^+ do show C_2 rotation, however.

Our simulation results for $Li(H_2O)_3$−hectorite, a system which has been studied extensively by spectroscopy, are in general agreement with the interpretation of both IR[2] and NMR[14] spectral data insofar as the average orientation of water molecules is concerned but differ sharply with the interpretation of these latter spectral data, as well as with QNS spectral data,[9,10] in respect to rotational motions. On the other hand, the Li^+ oscillations that were inferred as the cause of isotropicity in high-incident energy QNS spectra[9] are also predicted by our MD simulations. There is no agreement between our simulations and the spectroscopic models with regard to uniformity of the Li^+ solvation number or the type of surface complex formed. These major differences should be resolvable by constructing new spectroscopic models guided by the results presented in this paper and comparing them with extant or new spectral data.

Acknowledgment. The research reported in this paper was supported in part by NSF grant EAR 9505629 and in part by the Lawrence Berkeley National Laboratory under its LDRD program (Earth Sciences Division). The authors thank the Pittsburgh Supercomputer Center and the National Energy Research Scientific Computing Center for allocations of CPU time on Cray C90/J90 supercomputers. The authors express gratitude to Fang-Ru Chang, Columbia University, to Neal Skipper, University College London, and to Keith Refson, University of Oxford, for unfailing assistance with the MC/MD simulations. Thanks also to Sung-Ho Park, Rebecca Sutton, Satish Myneni, and two anonymous referees for their careful reviews and to Angela Zabel for excellent preparation of the manuscript.

References and Notes

(1) For a comprehensive discussion of clay mineral structure and composition, see: Weaver, C. E.; Pollard, L. D. *The Chemistry of Clay Minerals*; Elsevier: Amsterdam, 1973. Negative charge, created by the replacement of Mg^{2+} with Li^+ in the octahedral sheet, is balanced by interlayer Li^+ in hectorite.

(2) Prost, R. *Ann. Agron.* **1975**, *26*, 401, 463.

(3) (a) Sposito, G.; Prost, *R. Chem. Rev.* **1982**, *82*, 553. (b) Güven, N. Molecular aspects of clay/water interactions. In *Clay-Water Interface and its Rheological Implications*; Güven, N., Pollastro, R. M., Eds.; The Clay Minerals Society: Boulder, CO, 1992; p 1.

(4) Neilson, G. W.; Enderby, J. E. *Adv. Inorg. Chem.* **1989**, *34*, 195.

(5) Prost, R. *C. R. Acad. Sci. Paris* **1971**, *273*, 1467.

(6) Prost, R. In *Proceedings of the International Clay Conference*, México City, 1975; Bailey, S. W., Ed.; Applied Publishing Ltd.: Wilmette, IL, 1976; p 351.

(7) Poinsignon, C.; Cases, J. M.; Fripiat, J. J. *J. Phys. Chem.* **1978**, *82*, 1855.

(8) (a) Clementi, E.; Popkie, H. *J. Chem. Phys.* **1972**, *57*, 1077. (b) Feller, D.; Glendening, E. D.; Kendall, R. A.; Peterson, K. A. *J. Chem. Phys.* **1994**, *100*, 4981. (c) Marshall, C. L.; Nicholas, J. B.; Brand, H.; Carrado, K. A.; Winans, R. E. *J. Phys. Chem.* **1996**, *100*, 15748.

(9) Conard, J.; Estrade-Szwarckopf, H.; Dianoux, A. J.; Poinsignon, C. *J. Phys.* **1984**, *45*, 1361.

(10) Poinsignon, C.; Estrade-Szwarckopf, H.; Conard, J.; Dianoux, A. J. In *Proceedings of the International Clay Conference*, Denver, 1985; Schultz, L. G., van Olphen, H., Mumpton, F. A., Eds.; The Clay Minerals Society: Bloomington, IN, 1987; p 284.

(11) Ohtaki, H.; Radnai, T. *Chem. Rev.* **1993**, *93*, 1157.

(12) Conard, J. In *Proceedings of the International Clay Conference*, México City, 1975; Bailey, S. W., Ed.; Applied Publishing Ltd.: Wilmette, IL, 1976; p 221.

(13) Conard, J. *ACS Symp. Ser.* **1976**, *No. 34*, 85.

(14) Fripiat, J. J.; Kadi-Hanifi, M.; Conard, J.; Stone, W. E. E. In *Magnetic Resonance in Colloid and Interface Science*; Fraissard, J. P., Resing, H. A., Eds.; Reidel: Dordrecht, 1980; p 529.

(15) Luca, V.; Cardile, C. M.; Meinhold, R. H. *Clay Miner.* **1989**, *24*, 115.

(16) Mezei, M.; Beveridge, D. L. *J. Chem. Phys.* **1981**, *74*, 6902.

(17) Bopp, P. Molecular dynamics simulations of aqueous ionic solutions. In *The Physics and Chemistry of Aqueous Ionic Solutions*; Bellissent-Funel, M.-C., Neilson, G. W., Eds.; D. Reidel: Boston, MA, 1987; p 217.

(18) Allen, M. P.; Tildesley, D. J. *Computer Simulation of Liquids*; Clarendon Press: Oxford, 1987.

(19) Chang, F.-R. C.; Skipper, N. T.; Sposito, G. *Langmuir* **1997**, *13*, 2074.

(20) Chang, F.-R. C.; Skipper, N. T.; Sposito, G. *Langmuir* **1995**, *11*, 2734.

(21) Skipper, N. T.; Refson, K.; McConnell, J. D. C. *J. Chem. Phys.* **1991**, *94*, 7434.

(22) Skipper, N. T.; Refson, K.; McConnell, J. D. C. In *Geochemistry of Clay-Pore Fluid Interactions*; Manning, D. C., Hall, P. L., Hughs, C. R., Eds.; Chapman and Hall: London, 1993; p 40.

(23) Refson, K.; Skipper, N. T.; McConnell, J. D. C. In *Geochemistry of Clay-Pore Fluid Interactions*; Manning, D. C., Hall, P. L., Hughs, C. R., Eds.; Chapman and Hall: London, 1993; p 1.

(24) Skipper, N. T.; Chang, F.-R. C.; Sposito, G. *Clays Clay Miner.* **1995**, *43*, 285.

(25) Skipper N. T. *MONTE User's Manual;* Department of Physics and Astronomy, University College: London, 1996.

(26) Refson K. *MOLDY User's Manual;* Department of Earth Sciences, University of Oxford: Oxford, 1996.

(27) Calvet, R. *Ann. Agron.* **1973**, *24*, 77.

(28) Bérend, I.; Cases, J.-M.; François, M.; Uriot, J.-P.; Michot, L.; Masion, A.; Thomas, F. *Clays Clay Miner.* **1995**, *43*, 324.

(29) Skipper, N. T.; Sposito, G.; Chang, F.-R. C. *Clays Clay Miner.* **1995**, *43*, 294.

(30) Boek, E. S.; Coveney, P. V.; Skipper, N. T. *J. Am. Chem. Soc.* **1995**, *117*, 12608.